CrossMark

Ageing Scher–Montroll Transport

Henning Krüsemann[1] · Richard Schwarzl[1,2] ·
Ralf Metzler[1]

Abstract We study the properties of ageing Scher–Montroll transport in terms of a biased subdiffusive continuous time random walk in which the waiting times τ between consecutive jumps of the charge carriers are distributed according to the power law probability $\psi(t) \simeq t^{-1-\alpha}$ with $0 < \alpha < 1$. As we show, the dynamical properties of the Scher–Montroll transport depend on the ageing time span t_a between the initial preparation of the system and the start of the observation. The Scher–Montroll transport theory was originally shown to describe the photocurrent in amorphous solids in the presence of an external electric field, but it has since been used in many other fields of physical sciences, in particular also in the geophysical context for the description of the transport of tracer particles in subsurface aquifers. In the absence of ageing ($t_a = 0$) the photocurrent of the classical Scher–Montroll model or the breakthrough curves in the groundwater context exhibit a crossover between two power law regimes in time with the scaling exponents $\alpha - 1$ and $-1 - \alpha$. In the presence of ageing a new power law regime and an initial plateau regime of the current emerge. We derive the different power law regimes and crossover times of the ageing Scher–Montroll transport and show excellent agreement with simulations of the process. Experimental data of ageing Scher–Montroll transport in polymeric semiconductors are shown to agree well with the predictions of our theory.

1 Introduction

Anomalous diffusion, deviations from the laws of Brownian motion quantified by the diffusion equation (Fick's second law), was reported as early as 1935 by Freundlich and Krüger (1935) showing significant discrepancies from the predictions of Fick's laws in an analysis of

---

✉ Ralf Metzler
rmetzler@uni-potsdam.de

[1] Institute for Physics & Astronomy, University of Potsdam, 14476 Potsdam-Golm, Germany

[2] Physics Department, Free University of Berlin, 14195 Berlin, Germany

the 1914 experiments by Herzog and Polotzky (1914). Today, the term anomalous diffusion in statistical physics, biological physics, and geophysics refers to processes, whose mean squared displacement is no longer linear in time. Mostly, power laws of the form

$$\langle x^2(t) \rangle \simeq K_\alpha t^\alpha \tag{1}$$

are studied, where we distinguish between subdiffusion for the range $0 < \alpha < 1$ of the anomalous diffusion exponent and superdiffusion for $\alpha > 1$ (Metzler and Klafter 2000a; Bouchaud and Georges 1990). Equation (1) features the generalised diffusion coefficient K_α of physical dimension $[K_\alpha] = \mathrm{cm}^2/\mathrm{s}^\alpha$. This unusual dimensionality can be understood from physical models as discussed below.

Anomalous diffusion in the sense of Equation (1) was first reported by Richardson (1926) for the relative diffusion of two tracer particles in turbulent flows. In condensed matter physics possibly the most influential paper on anomalous diffusion is the work on the *dispersive* transport of charge carrier motion in amorphous semiconductors by Scher and Montroll (1975), containing the subdiffusive formulation of the Weiss–Montroll continuous time random walk (Montroll and Weiss 1965; Shlesinger 1974). In a geophysical context, anomalous diffusion occurs frequently in the spreading of tracer chemicals in aquifers (Berkowitz et al. 2006; Kirchner et al. 2000). Today, modern microscopic techniques unveil subdiffusion of artificial and endogenous tracer particles of submicron size in living biological cells (Weiss et al. 2004; Jeon et al. 2011, 2013b; Golding and Cox 2006; Kepten et al. 2011; Barkai et al. 2012) and complex (crowded) liquids (Habdas et al. 2004; Tejedor et al. 2010; Szymanski and Weiss 2009). Recent advances in superresolution microscopy even allow experimentalists to measure anomalous diffusion of nanometre-sized fluorescent molecules in live cells (Di Rienzo et al. 2014) or of single lipid molecules in biological membranes at nanosecond time scales (Honigmann et al. 2013). Due to active, energy-consuming processes in living cells, also superdiffusion has been measured (Caspi et al. 2000; Robert et al. 2010; Reverey et al. 2015).

Ageing is a well-known phenomenon in glass-forming systems, namely after a temperature quench glassy systems exhibit an explicit dependence not only on the probing time but also on the ageing time elapsing between the quench and the start of the probing experiment (Henkel et al. 2007; Donth 2001). Monthus and Bouchaud (1996) showed that such ageing can be understood in terms of quenched trap models with exponential distributions of well depths, leading to diverging waiting time scales below a (glass) temperature (Bouchaud and Georges 1990). In these models a tracer particle on average falls into ever deeper traps, and thus, its effective mobility decreases with time. However, even in living biological cells ageing was found to govern the diffusive dynamics of channel proteins in cellular membranes (Weigel et al. 2011; Manzo et al. 2014) as well as the motion in the cellular cytoplasm of insulin granules (Tabei et al. 2013). Another example for ageing dynamics comes from cooling granular gases in the homogeneous phase (Bodrova et al. 2015) and semiclassical systems (Brokmann et al. 2003).

In particular, ageing is observed for the Scher–Montroll transport of charge carriers in polymeric semiconductors (Schubert et al. 2013). Experimentally, the ageing behaviour of the charge carriers is probed as follows: charge carriers are generated by a light flash and then allowed to subdiffuse freely in the semiconductor. After the ageing time t_a an external electrical driving field is switched on, and then the Scher–Montroll current recorded in time-of-flight measurements (Schubert et al. 2013). Indeed, the experiments reveal a significant modification of the current-time characteristic compared to non-aged, classical Scher–Montroll transport, as evidenced in Fig. 1. Similar situations could be envisaged in a geophysical context: imagine that some chemical tracer is spilled and allowed to mix locally in the

Fig. 1 Electrical current in time-of-flight experiments in polymeric semiconductors (Schubert et al. 2013). In the absence of ageing (ToF) the classical Scher–Montroll result with two power laws is displayed. When the system is aged (td-ToF), the current characteristic changes and as shown by extrapolations based on Monte Carlo simulations an initial current plateau emerges (Schubert et al. 2013)
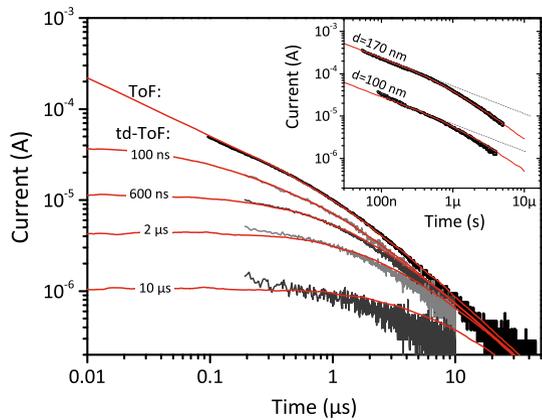
groundwater aquifer, which was shown to be characterised by continuous time random walk-like transport (Berkowitz et al. 2006; Berkowitz and Scher 1997). After an ageing period t_a a bias flow is caused by a period of rainfall. Effects on the dispersive transport of the tracer similar to the observations in the semiconductor would be expected.

Here we extend the work of Barkai and Cheng (2003) and Barkai (2003) on the description of ageing Scher–Montroll behaviour and our results on ageing first passage behaviour in subdiffusive continuous time random walk processes (Krüsemann et al. 2014, 2015) to obtain the full analytical behaviour of the ageing Scher–Montroll dynamics. In particular, we demonstrate the emergence of an initial plateau in the current-time characteristic and show that the predicted scaling of the plateau value is in good agreement with experimental results from charge carrier motion in polymeric semiconductors. Throughout the article, the wording will be based on the concept of an electric current, but we stress that it is equivalent to the current of tracer particles in groundwater breakthrough experiments.

2 Subdiffusive Continuous Time Random Walks and Ageing Dynamics

Anomalous transport processes based on stationary increments such as fractional Brownian motion or fractional Langevin motion (Mandelbrot and van Ness 1968; Goychuk 2012) are at most transiently ageing (Kursawe et al. 2013). Ageing is indeed related to the non-stationary nature of the process. While this includes Markovian processes with explicitly space (Cherstvy and Metzler 2015) or time (Jeon et al. 2014) dependent diffusion coefficients, the classical example is that of subdiffusive continuous time random walks (CTRWs). This model, originally propagated by Scher and Montroll (1975) and Shlesinger (1974), is based on a random walk process, in which successive jumps are separated by a random waiting time distributed in terms of a waiting time density with power law tail

$$\psi(\tau) \simeq \frac{\tau_0^\alpha}{\tau^{1+\alpha}}, \tag{2}$$

where $\alpha > 0$ and τ_0 is a scaling factor of unit $[\tau_0] = $ sec. When $0 < \alpha < 1$, the characteristic waiting time $\langle \delta\tau \rangle = \int^\infty \tau \psi(\tau) d\tau$ diverges and the dynamics becomes subdiffusive with mean squared displacement (1). In the sense of the quenched energy landscape model this

case would correspond to a system temperature below the glass temperature (Bouchaud and Georges 1990; Monthus and Bouchaud 1996).

Indeed, power law waiting time distributions can be directly monitored on the basis of individual trajectories of protein channels in cellular membranes (Weigel et al. 2011), the motion of submicron tracers in gels of semiflexible filaments (Wong et al. 2004) and of functionalised submicron tracers in the vicinity of complementarily functionalised surfaces (Xu et al. 2011). Moreover, simulations show that a power law waiting time density can be reconstructed from the distribution of hydraulic conductivities in porous systems (Edery et al. 2014). The full immobilisation of a tracer particle in a trapped state in experiments may be masked by additional environmental noise (Jeon et al. 2013a). CTRW-like motion was also shown to be associated with submicron granule motion in living biological cells (Jeon et al. 2013b; Tabei et al. 2013). Subdiffusive CTRWs are also underlying the tracer particle motion in porous structures in subsurface aquifers (Berkowitz et al. 2000, 2002) and even the blinking dynamics of quantum dots (Brokmann et al. 2003; Jung et al. 2002) and their arrays (Sibatov 2011). We note that in an external force field subdiffusive CTRWs are conveniently described in terms of the fractional Fokker–Planck equation (Barkai 2001; Metzler et al. 1999; Metzler and Klafter 2000a).

After the original studies by Monthus and Bouchaud (1996) and Bouchaud and Georges (1990) the ageing behaviour of subdiffusive CTRWs was explored by Barkai and Cheng (2003) and Barkai (2003); see also the recent perspective article on ageing CTRW motion and renewal theory (Schulz et al. 2014). The existence of ageing was also demonstrated in dynamic maps (Akimoto and Barkai 2013; Barkai 2003). The ageing-related effect of a weakening response to an external sinusoidal driving was revealed in subdiffusive CTRWs (Sokolov and Klafter 2006) and correlated CTRWs (Magdziarz et al. 2012). Generally, the occurrence of an additional time scale specified by t_a gives rise to characteristic crossover behaviours of physical observables. For instance, the mean squared displacement of an unconfined ageing subdiffusive CTRW process reads (Barkai and Cheng 2003; Barkai 2003; Schulz et al. 2014)

$$\langle x_a^2(t) \rangle = \langle [x^2(t) - x(t_a)]^2 \rangle \begin{cases} \dfrac{t^\alpha}{\Gamma(1+\alpha)} + \dfrac{t_a^\alpha}{\Gamma(1-\alpha)}, \ t_a \ll t \\ \dfrac{t_a^{\alpha-1} t}{\Gamma(\alpha)}, \qquad\qquad\qquad t_a \gg t \end{cases}, \qquad (3)$$

where by convention we count the time t from the end of the ageing period t_a. For weak ageing when $t \gg t_a$ a correction term emerges in the mean squared displacement. For strong ageing with $t_a \gg t$ the leading term is, deceivingly, linear and suggests normally diffusive behaviour, with a correction factor $t_a^{\alpha-1}$. Interestingly, for the corresponding time averaged mean squared displacement the scaling in terms of the dynamical variable remains unchanged in the presence of even strong ageing, the effect of t_a entering solely in terms of a multiplicative ageing prefactor (Schulz et al. 2013, 2014). Analogously, ageing-caused crossovers were also observed in the first passage density of subdiffusive CTRW processes (Krüsemann et al. 2014, 2015). A significant feature of ageing CTRW motion is the splitting up of a population of tracer particles into a discrete immobile fraction and a distributed, mobile fraction during finite observation periods (Schulz et al. 2013, 2014). We note that a similar feature arises in strongly varying diffusivity fields (Metzler et al. 2014; Cherstvy and Metzler 2013).

The ageing behaviour of subdiffusive CTRWs is related to weakly non-ergodic dynamics (Metzler et al. 2014; Bouchaud 1992; Bel and Barkai 2005; Lubelski et al. 2008; He et al. 2008) according to which even in the long measurement time limit the ensemble and time averages of physical observables such as the mean squared displacement do not converge.

This phenomenon is also related to modifications of the Khinchin theorem (Burov et al. 2010). We also mention that certain ageing effects also occur in the range $1 < \alpha < 2$ when we encounter a finite characteristic waiting time $\langle \delta \tau \rangle$ but infinite fluctuations $\langle \delta \tau^2 \rangle$ (Allegrini et al. 2002).

3 Ageing Scher–Montroll Transport: Biased Continuous Time Random Walks

We consider the Scher–Montroll scenario with power law waiting time density (2) and the initial distribution of the test particle's position,

$$p_0(x) = \frac{1}{b} \left[\Theta \left(x + b/2 \right) - \Theta \left(x - b/2 \right) \right], \tag{4}$$

of width b in the semi-infinite domain $(-\infty, a)$, with $a > b$. The rescaled force

$$B = \frac{F}{2k_B T}, \tag{5}$$

corresponding to the external electric field in the context of Scher–Montroll charge carrier transport or the water drift in the geophysical setting, drives the walker towards the absorbing boundary (counter-electrode, catchment) located at $x = a$ such that $P(a, t) = 0$. Note that in what follows we denote the Laplace transform of a function by its explicit dependence on the Laplace variable u,

$$f(u) = \int_0^\infty e^{-ut} f(t) \mathrm{d}t. \tag{6}$$

Introducing the abbreviations

$$A = 2u^{\alpha-1}(\tau^\star)^\alpha, \ \ C = \sqrt{1 + 4(u\tau^\star)^\alpha}, \tag{7}$$

and the time scale

$$\tau^\star = (4B^2 K_\alpha)^{-1/\alpha}, \tag{8}$$

we write the non-aged, unconfined probability density function as (Barkai 2001)

$$P(x, u) = \frac{AB}{C} \exp \left(B \left[x - C|x| \right] \right). \tag{9}$$

The ageing probability density is then given by Barkai and Cheng (2003), Barkai (2003), Schulz et al. (2014), and Schulz et al. (2013)

$$P(x, s, u) = P_0(s, u) p_0(x) + h(s, u) P(x, u) \otimes p_0(x), \tag{10}$$

where $P_0(t_a, t)$ is the probability density of not having made a step until time t after the ageing period of duration t_a, while $h(t_a, t)$ is the density of the forward waiting or recurrence time one has to wait for the first step to occur after the initial ageing period (Godrèche and Luck 2001). Moreover, s is the Laplace space variable corresponding to t_a and the symbol $\otimes$ is defined as

$$P(x, u) \otimes p_0(x) = \int\limits_{-\infty}^{\infty} P(x', u) p_0(x - x') \mathrm{d}x'. \tag{11}$$

We note that the statistic of h is different from that of the original ψ: for increasing ageing period the likelihood increases that the system at the start of the measurement is locked in a

very long trapping event, rendering the relative contribution of the factor $P_0(t_a, t)$ ever more relevant.

The solution for the semi-infinite geometry with an absorbing boundary is found using the method of images (Barkai 2001; Metzler and Klafter 2000b)

$$\hat{P}(x, s, u) = P(x, s, u) - \mathcal{M} P(x - 2a, s, u), \qquad (12)$$

with the boundary condition $\hat{P}(a, s, u) = 0$. The solution $\hat{P}(x, t, t_a)$ is no longer a probability density function (PDF), as its norm decays with time. To balance for the drift when we apply the method of images, we introduced above the proportionality coefficient

$$\mathcal{M} = \frac{P(x, u) \otimes p_0(x)|_a}{P(x, u) \otimes p_0(x)|_{-a}}. \qquad (13)$$

The convolution term introduced in Eq. (10) features the three regimes

$$
\begin{aligned}
&P(x, u) \otimes p_0(x) \\
&= \frac{A}{bC} \begin{cases} 2 \exp\left(Bx[1 + C]\right) \sinh\left(Bb[1 + C]/2\right)/(1 + C), & x < -b/2 \\ \left[\exp\left(B[1 - C][x + b/2]\right) - 1\right]/(1 - C) \\ \quad + \left[1 - \exp\left(B[1 + C](x - b/2)\right)\right]/(1 + C), & -b/2 < x < b/2 \\ 2 \exp\left(Bx[1 - C]\right) \sinh\left(Bb[1 - C]/2\right)/(1 - C), & x > b/2 \end{cases}
\end{aligned}
\qquad (14)
$$

and the image factor depending on the position x with respect to $\pm b/2$ assumes the explicit form

$$\mathcal{M} = \exp\left(2Ba\right) \frac{\exp\left(Bb[1 - C]/2\right) - \exp\left(-Bb[1 - C]/2\right)}{\exp\left(Bb[1 + C]/2\right) - \exp\left(-Bb[1 + C]/2\right)} \frac{1 + C}{1 - C}. \qquad (15)$$

An important quantity in the calculation of the Scher–Montroll current is the survival. It measures the probability that a given charge carrier has not yet been absorbed by the counter-electrode. This survival probability is given by

$$\mathcal{S}(s, u) = \int\limits_{-\infty}^{a} \hat{P}(x, s, u) \mathrm{d}x. \qquad (16)$$

After some linear transformations of the integration variable (note that $a > b/2$) we find the result

$$\mathcal{S}(s, u) = P_0(s, u) + h(s, u) \left(\int_{-\infty}^{-b/2} \mathrm{I}(x) \mathrm{d}x + \int_{-b/2}^{b/2} \mathrm{II}(x) \mathrm{d}x \right.$$
$$\left. + \int_{b/2}^{a} \mathrm{III}(x) \mathrm{d}x - \mathcal{M} \int_{-\infty}^{-a} \mathrm{I}(x) \mathrm{d}x \right). \qquad (17)$$

The Roman numerals stand for the three regimes of equation (14), respectively. The integral of $\mathrm{II}(x)$ can be separated,

$$\int_{-b/2}^{b/2} \mathrm{II}(x) \mathrm{d}x = \frac{2A}{C^2 - 1} + \int_{0}^{b} {}^{-}\mathrm{II}(x) \mathrm{d}x - \int_{-b}^{0} {}^{+}\mathrm{II}(x) \mathrm{d}x, \qquad (18)$$

where we abbreviated

$${}^{\mp}\mathrm{II}(x) = \frac{A}{bC(1 \mp C)} \exp\left(B[1 \mp C]x\right). \qquad (19)$$

Another important quantity in the Scher–Montroll model is the average position of the remaining (non-absorbed) particles

$$\langle x(s, u)\rangle_r = \int_{-\infty}^{a} x \hat{P}(x, s, u)\mathrm{d}x. \tag{20}$$

We use coordinate shifts and integration by parts and obtain

$$\langle x(s, u)\rangle_r = h(s, u)\left\{-\mathcal{M}\left(\left[2a - \frac{1}{B(1+C)}\right]\int_{-\infty}^{-a}\mathrm{I}(x)\mathrm{d}x + \frac{1}{B(1+C)}\left[x\mathrm{I}(x)\right]_{-\infty}^{-a}\right)\right.$$
$$-\frac{1}{B(1+C)}\int_{-\infty}^{-b/2}\mathrm{I}(x)\mathrm{d}x + \frac{1}{B(1+C)}\left[x\mathrm{I}(x)\right]_{-\infty}^{-b/2}$$
$$+\left(\frac{1}{B(1+C)} - \frac{b}{2}\right)\int_{-b}^{0}{}^{+}\mathrm{II}(x)\mathrm{d}x - \left(\frac{1}{B(1-C)} + \frac{b}{2}\right)\int_{0}^{b}{}^{-}\mathrm{II}(x)\mathrm{d}x$$
$$-\frac{1}{B(1+C)}\left[x\mathrm{I}(x)\right]_{-b}^{0}\sinh\left(\frac{Bb[1+C]}{2}\right)$$
$$+\frac{1}{B(1+C)}\left[x\mathrm{III}(x)\right]_{0}^{b}\sinh\left(\frac{Bb[1-C]}{2}\right)$$
$$+\frac{1}{B(1+C)}\left[x\mathrm{I}(x)\right]_{b/2}^{a} - \frac{1}{B(1-C)}\int_{b/2}^{a}\mathrm{III}(x)\mathrm{d}x\right\}, \tag{21}$$

where $\left[x\mathrm{I}(x)\right]_{l}^{u}$ is defined as the product of x and the Roman numeral, evaluated at the upper and lower values,

$$\left[x\mathrm{I}(x)\right]_{l}^{u} = u \times \mathrm{I}(u) - l \times \mathrm{I}(l) \tag{22}$$

The overall mean $\langle x(t, t_a)\rangle$ is a combination of the average of the remaining particles and the share of the absorbed walkers that accumulate at the counter-electrode (catchment) located at $x = a$,

$$\langle x(s, u)\rangle = \langle x(s, u)\rangle_r + a\left(\frac{1}{su} - \mathscr{S}(s, u)\right). \tag{23}$$

Substituting the solutions, evaluating the integrals, using the property (Schulz et al. 2014)

$$P_0(s, u) = \frac{1 - sh(s, u)}{su}, \tag{24}$$

and by help of the additional abbreviations

$$D = \frac{A}{BbC[1+C]^2}, \quad E = \frac{A}{BbC[1-c]^2} \tag{25}$$

we obtain

$$\langle x(s, u)\rangle = h(s, u)\left\{\frac{a}{u} - \frac{2Aa}{C^2 - 1} + \exp\left[B(1+C)(b/2 - a)\right]\mathcal{M}D\left(-a + \frac{1}{B(1+C)} + a\right)\right.$$
$$+ \exp\left[B(1+C)(-b/2 - a)\right]\mathcal{M}D\left(a - \frac{1}{B(1+C)} - a\right) + \exp\left[-B(1+C)b\right]D$$
$$\times\left[a + \frac{1}{B(1+C)} + b/2 - a - \frac{1}{B(1+C)} + b/2 - b\right]$$

$$+D\left[-a - \frac{1}{B(1+C)} - b/2\right] + E\left[a + b/2 + \frac{1}{B(1-C)}\right]$$

$$+D\left[a - b/2 + \frac{1}{B(1+C)}\right] + E\left[-a - \frac{1}{B(1-C)} + b/2\right]$$

$$+\exp[B(1-C)b]E\left[-a + b/2 - \frac{1}{B(1-C)} + a + \frac{1}{B(1-C)} - b/2 + b\right]$$

$$+\exp[B(1-C)(a+b/2)]E\left[-a - \frac{1}{B(1-C)} + a\right]$$

$$+\exp[B(1-C)(a-b/2)]E\left[a + \frac{1}{B(1-C)} - a\right]\bigg\}. \tag{26}$$

Here we sorted the results by exponential functions and did not cancel obvious terms to point out the origins of the various terms. We now simplify further, using the property that

$$\frac{a}{u} = \frac{2Aa}{C^2 - 1}, \quad b(E - D) = \frac{4A}{B(1 - C^2)^2} \tag{27}$$

so that we obtain

$$\langle x(s,u)\rangle = h(s,u)\left\{\left[-\exp(B[1-C][a+b/2]) + \exp(B[1-C][a-b/2])\right]\right.$$

$$+ \frac{D\mathcal{M}}{B(1+C)}\left[\exp(B[1+C][-a+b/2]) - \exp(B[1+C][-a-b/2])\right]$$

$$\left. + \frac{4A}{B(1-C^2)^2} + \frac{E}{B(1-C)}\right\}. \tag{28}$$

We insert the expression for $\mathcal{M}$ and reorganise the terms,

$$\langle x(s,u)\rangle = h(s,u)\left\{\frac{\exp[B(1-C)(a+b/2)]}{Bb(1-C)}\left(-E + D\frac{1 - \exp[-Bb(1-C)]}{1 - \exp[-Bb(1+C)]}\right)\right.$$

$$+ \frac{\exp[B(1-C)(a-b/2)]}{Bb(1-C)}\left(E - D\frac{\exp[Bb(1-C)] - 1}{\exp[Bb(1+C)] - 1}\right)$$

$$\left. + \frac{4A}{B(1-C^2)^2}\right\} \tag{29}$$

$$= h(s,u)\left\{\frac{A\exp(B[1-C]a)}{B^2Cb(1-C)}\left[\exp(-Bb[1-C]/2) - \exp(Bb[1-C]/2)\right]\right.$$

$$\times\frac{1}{(1-C)^2}\left[1 - \frac{1}{1 - \exp(-Bb[1+C])} - \frac{1}{1 - \exp(Bb[1+C])}\right]$$

$$\left. + \frac{4A}{B(1-C^2)^2}\right\}$$

$$= h(s,u)\frac{4A}{B(1-C^2)^2}\left(1 + \frac{\exp(B[1-C]a)}{Bb(1-C)}\left[\exp(-Bb[1-C]/2)\right.\right.$$

$$\left.\left. - \exp(Bb[1-C]/2)\right]\right). \tag{30}$$

In the amorphous semiconductor example the current induced by the hopping charge carriers is proportional to the diffusive/dispersive velocity of the charge carriers and can thus be derived directly from the mean. Using the Laplace transform of the time derivative we find that (Scher and Montroll 1975; Barkai 2001)

$$I(s,u) \simeq \langle v(s,u)\rangle \sim u\,\langle x(s,u)\rangle. \tag{31}$$

We will employ this relation below.

3.1 Recovering the Result for Initial δ-Distribution

As it requires some care to show the relation of the above result for a spread out initial condition with that for a sharp initial condition $p_0(x) = \delta(x)$ we briefly show here the consistency of the results in the limit of vanishing width b. Indeed, for small b values one finds

$$\left[\exp\left(-Bb[1-C]/2\right) - \exp\left(Bb[1-C]/2\right)\right]/[Bb(1-C)]$$
$$= -1 + \mathcal{O}(b^2), \tag{32}$$

where $\mathcal{O}(b^2)$ denotes terms of order b^2. The current for $b \to 0$ is

$$I_{\delta,0}(s,u) \sim uh(s,u)\frac{4A}{B(1-C^2)^2}\left(1 - \exp\left(B[1-C]a\right)\right). \tag{33}$$

To prove that this is indeed the correct form, we note that starting from an initial δ distribution, one can find the result for the step initial condition in a more simple manner. If we shift the initial peak from $x = 0$ to a more general position $x = x_0$, the result will be the same, only that $a \to a - x_0$ is shifted, since the peak gets closer to the absorbing boundary. We can now convolve our Green's function with the initial step and find

$$I(s,u) = I_{\delta,x_0}(s,u) \otimes \left(b^{-1}\left[\Theta\left(x - b/2\right) - \Theta\left(x + b/2\right)\right]\right)$$
$$= b^{-1}\int_{-b/2}^{b/2} I_{\delta,x_0}(s,u)\mathrm{d}x_0$$
$$\sim b^{-1}\int_{-b/2}^{b/2} uh(s,u)\frac{4A}{B(1-C^2)^2}\left(1 - \exp\left(B[1-C](a - x_0)\right)\right)$$
$$= \left[1 - \exp\left(B[1-C]a\right)\left(\frac{\exp\left(B(1-C)b/2\right) - \exp\left(-B(1-C)b/2\right)}{Bb(1-C)}\right)\right]$$
$$\times \frac{4Auh(s,u)}{B(1-C^2)^2}, \tag{34}$$

which indeed matches Eq. (30) inserted into Eq. (31).

4 Long Time Behaviour

Instead of directly analysing the long time behaviour of the current, it is more convenient to inspect the small u behaviour in Laplace space and invert these terms using Tauberian theorems (Davies 2002; Feller 1971)—the dominant terms in the limit $u \to 0$ correspond to the leading terms as $t \to \infty$. For our expansion we use the variable $q = 4(u\tau^\star)^\alpha$ as the small parameter. The following relations are exact:

$$uA = q/2, \quad C = \sqrt{1+q}, \quad 1 - C^2 = -q. \tag{35}$$

Expansion for small values of q yields

$$\exp\left(-Bb[1-C]/2\right) - \exp\left(Bb[1-C]/2\right)$$
$$\approx \left(1 + \frac{Bb}{4}q + \frac{1}{8}\left[\frac{B^2b^2}{4} - \frac{Bb}{2}\right]q^2 + \frac{1}{48}\left[\frac{B^3b^3}{8} - \frac{3B^2b^2}{4} + \frac{3Bb}{2}\right]q^3\right)$$
$$- \left(1 - \frac{Bb}{4}q + \frac{1}{8}\left[\frac{B^2b^2}{4} + \frac{Bb}{2}\right]q^2 + \frac{1}{48}\left[-\frac{B^3b^3}{8} - \frac{3B^2b^2}{4} - \frac{3Bb}{2}\right]q^3\right)$$
$$= \frac{1}{2}Bbq\left[1 - \frac{q}{4} + \frac{q^2}{8}\left(1 + \frac{B^2b^2}{12}\right)\right]. \tag{36}$$

Moreover,

$$(1-C)^{-1} \approx \frac{2}{q}\left(1 + \frac{q}{4} - \frac{q^2}{16}\right) \tag{37}$$

and

$$\exp\left(Ba[1-C]\right) \approx 1 - \frac{Ba}{2}q + \frac{q^2}{8}\left[B^2a^2 + Ba\right]. \tag{38}$$

Thus, we arrive at the following asymptotic behaviour for the electrical current in Laplace space,

$$I(u) \sim h(s,u)\left\{\frac{2q}{Bq^2}\left[1 - \left(1 - \frac{Ba}{2}q + \frac{q^2}{8}\left[B^2a^2 + Ba\right]\right)\right.\right.$$
$$\left.\left. \times \frac{2}{q}\left(1 + \frac{q}{4} - \frac{q^2}{16}\right)\frac{1}{2}Bbq\left(1 - \frac{q}{4} + \frac{q^2}{8}\left[1 + \frac{B^2b^2}{12}\right]\right)\middle/Bb\right]\right\}$$
$$= h(s,u)\left[a - \left(\frac{a}{4}(1+Ba) + \frac{Bb^2}{48}\right)q + \mathcal{O}(q^2)\right], \tag{39}$$

where the symbol $\mathcal{O}(q^2)$ denotes terms of order q^2. If we compare in this result the contribution of the δ initial condition with that containing the width,

$$h(s,u)\frac{Bb^2}{48}q, \tag{40}$$

we find that this is negligible, since it has to be compared to the term

$$h(s,u)\frac{Ba^2}{4}q, \tag{41}$$

where $a > b$. The asymptotic behaviour is thus independent of the finite width of the initial conditions, as it should.

4.1 Freely Subdiffusing Biased Particle (Dispersive Transport)

If the barrier is sufficiently far away, the current will for shorter—but still sufficiently long—times be dominated by the long time behaviour of a biased diffusion without boundary. The boundary effects only play a role when the mean of the distribution has reached the boundary. This is the reason for the two regimes in the Scher–Montroll transport (Scher and Montroll 1975). The mean of unbounded biased subdiffusion starting from the initial condition $p_0(x) = \delta(x - x_0)$ is (Barkai and Cheng 2003)

$$\langle x(s,u)\rangle = x_0 + \frac{h(s,u)}{2B}u^{-\alpha-1}\tau^{-\alpha}. \tag{42}$$

The convolution with the step initial condition just eliminates the value x_0, as the step is symmetric around zero. The initial current in the Scher–Montroll transport thus follows in the form

$$I_I(s, u) \sim \frac{h(s, u)}{2B}(u\tau)^{-\alpha}.$$ (43)

This result was derived previously by Barkai and Cheng (2003).

5 Scaling Regimes in Ageing Scher–Montroll Transport

We now expand the forward waiting time density to find the leading order results for the Scher–Montroll current in different regimes defined by combinations of the relevant time scales. The exact form for a subdiffusive CTRW in Laplace space is (Schulz et al. 2014)

$$h(t_a, u) = \exp(ut_a)\frac{\Gamma(\alpha, t_a u)}{\Gamma(\alpha)}.$$ (44)

We need to consider two cases, since the incomplete Gamma function has two different expansions when the second argument tends to infinity or to zero (Krüsemann et al. 2015). For strong ageing ($t_a \gg t$) the product $ut_a \to \infty$ and the forward waiting time density becomes

$$h(t_a, u) \sim \frac{(ut_a)^{\alpha-1}}{\Gamma(\alpha)}.$$ (45)

For weak ageing ($t_a \ll t$) the product tends to zero and the result is

$$h(t_a, u) \sim 1 - \frac{(t_a u)^\alpha}{\Gamma(1+\alpha)}.$$ (46)

If we plug this into expressions (39) and (43), setting $b = 0$ for a δ initial condition for the PDF, and reinsert $q = 4(u\tau^\star)^\alpha$ we find

$$I_I(t_a, t) \sim \frac{k_B T}{F(\tau^\star)^\alpha}\frac{t_a^{\alpha-1}}{\Gamma(\alpha)}$$ (47)

$$I(t_a, t) \sim a\frac{t_a^{\alpha-1}t^{-\alpha}}{\Gamma(\alpha)\Gamma(1-\alpha)}$$ (48)

for strong ageing ($t_a \gg t$) and

$$I_I(t_a, t) \sim \frac{k_B T}{F(\tau^\star)^\alpha}\frac{t^{\alpha-1}}{\Gamma(\alpha)}$$ (49)

$$I(t_a, t) \sim \left[a\alpha(\tau^\star)^\alpha + \frac{a^2\alpha F(\tau^\star)^\alpha}{2k_B T} + \frac{a\alpha t_a^\alpha}{\Gamma[1+\alpha]}\right]\frac{t^{-1-\alpha}}{\Gamma(1-\alpha)}$$ (50)

for weak ageing ($t_a \ll t$).

The transition from the initial (I_I) to the final behaviour (I) occurs at the classical crossover time (Barkai 2001)

$$t_c = \left[\frac{\Gamma(1+\alpha)}{2\Gamma(1-\alpha)}\right]^{1/2\alpha}\left(\frac{a}{2BK_\alpha}\right)^{1/\alpha}.$$ (51)

Here t_c is defined as the time when the mean of the distribution of charge carriers has reached the boundary at $x = a$. In a strongly aged system a large part of the diffusing particles is immobile (Schulz et al. 2013, 2014). The current is generated solely by the mobile part,

which behaves like the non-aged system so that the crossover at t_c also characterises the aged system. Depending on the value of t_c and the ageing time t_a the current undergoes one or two crossovers between the above regimes. Using the definition (8) for the time scale $\tau^\star$ we find the following regimes

$$
I(t_a, t) \sim
\begin{cases}
\dfrac{F K_\alpha}{k_B T} \dfrac{t_a^{\alpha-1}}{\Gamma(\alpha)}, & t \ll t_a, t_c \\[3mm]
\dfrac{F K_\alpha}{k_B T} \dfrac{t^{\alpha-1}}{\Gamma(\alpha)}, & t_a \ll t \ll t_c \\[3mm]
a \dfrac{t_a^{\alpha-1} t^{-\alpha}}{\Gamma(\alpha)\Gamma(1-\alpha)}, & t_c \ll t \ll t_a \\[3mm]
\left[\dfrac{a\alpha(k_B T)^2}{F^2 K_\alpha} + \dfrac{a^2\alpha k_B T}{2 F K_\alpha} + \dfrac{a\alpha t_a^\alpha}{\Gamma[1+\alpha]} \right] \dfrac{t^{-1-\alpha}}{\Gamma(1-\alpha)}, & t \gg t_a, t_c
\end{cases}
. \tag{52}
$$

This detailed crossover behaviour is the main result of this work. The initial plateau regime was already mentioned by Barkai and Cheng (2003). The second and the fourth regimes are the slightly modified standard Scher–Montroll power laws for non-ageing systems. The third regime is given directly by the forward waiting time density at long ageing times, while both ageing regimes reflect the fact that the first step in an ageing CTRW only occurs after a power law waiting time drawn from $h(t_a, t)$. Apart from this additional scaling regime what is new here is the explicit calculation of the coefficients in the four power law regimes. Furthermore, depending on the times t_a, t_c, and the observation time window, we can now predict up to two crossovers between different power law regimes in a single Scher–Montroll experiment.

6 Numerical Simulation

Using Mathematica (Wolfram 1991) we calculated the derivative of the mean position, $\frac{d}{dt} \langle x(t_a, t) \rangle$ numerically, based on the exact expression

$$
u \langle x(t_a, u) \rangle = u \exp(t_a u) \Gamma(\alpha, t_a u) \Gamma^{-1}(\alpha)
$$
$$
\times \frac{4A}{B(1-C^2)^2} \left(1 - \exp(B[1-C]a) \right) \tag{53}
$$

in Laplace space for the δ initial condition, given by Eqs. (33) and (44). The Laplace inversion $(u \to t)$ is performed using the Mathematica function GWR. As predicted, the four panels in Fig. 2 exhibit the appearance of two or three different power law regimes and the plateau in the current characteristic (52), depending on the values of the relevant time scales t_a and t_c. We find the two classical Scher–Montroll regimes in the non-ageing case when t_a is zero, as demonstrated in the top left of Fig. 2. In the case when $t_a = t_c$ leaving only a single characteristic time, the plateau crosses over directly to the final power law, as shown in the bottom left panel of Fig. 2. For $t_a \ll t_c$ and $t_a \gg t_c$ we observed the predicted three regimes, as shown in the two right panels in Fig. 2.

In the ageing current characteristics shown in the top right and the two bottom panels of Fig. 2 we see the constant initial plateau. The value of this plateau decays as a power law of the ageing time t_a, as given by Eq. (47). We calculated the value $I(t = 500)$ of the current at $t = 500$ for different values of t_a and find good agreement with Eq. (47), as demonstrated in Fig. 3.

We also consider the case of a broad initial distribution of width b which leads to the Scher–Montroll current described by Eq. (39) in the long time limit. We find that the difference to
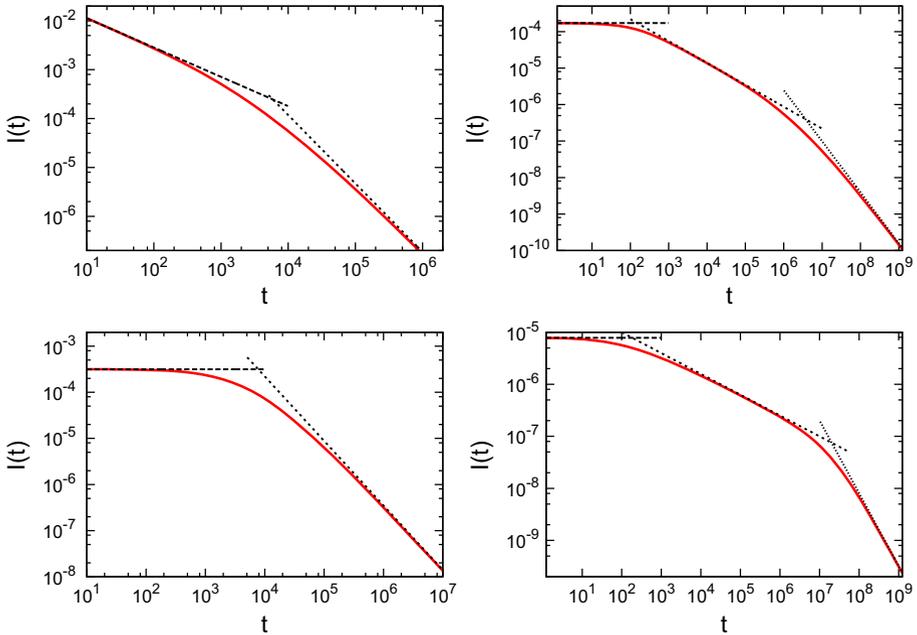
Fig. 2 Scher–Montroll current $I(t)$ for different values of the ageing time t_a and the crossover time t_c for $\alpha = 2/5$. *Top left*: $t_a = 0$, $t_c = 3890$. *Top right*: $t_a = 150$, $t_c = 2.37 \times 10^6$. *Bottom left*: $t_a = t_c = 3890$. *Bottom right*: $t_a = 2 \times 10^7$, $t_c = 110$

Fig. 3 Initial plateau value (*red line*) of the Scher–Montroll current at $t = 500$ as function of the ageing time t_a from exact Laplace inversion. The *black dashed line* is the theoretical power law (47)
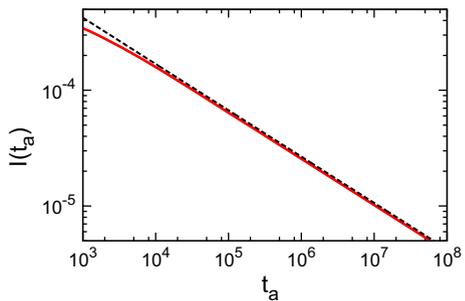
the current produced by an initial δ distribution is only marginal in the long time limit, as shown in Sect. 3. Figure 4 corroborates numerically that both cases lead to almost identical current characteristic in this long time limit. Since the difference is invisible in this graph, we also show the non-normalised difference on the right of Fig. 4 and find that the behaviour is indeed given by the power law term (40).

7 Experimental Ageing Scher–Montroll Current

The relevance of our calculations from an experimental point of view is shown by the Scher–Montroll current characteristic shown in Fig. 1. In the underlying experiment time-of-flight measurements are performed in a dioctyl substituted copolymer PFTBTT (alt-PF8TBTT)
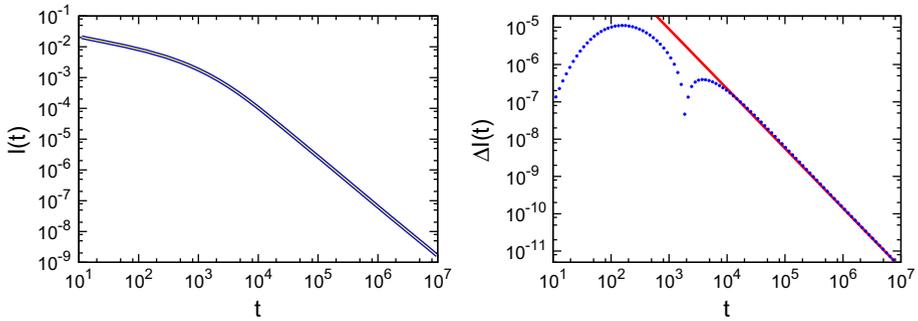
Fig. 4 Scher–Montroll current for initial widths $b = a/5$ (*blue*) and $b = 0$ (*yellow*) of the charge carrier distribution, for $B = 1/5$, $\alpha = 3/5$, $K_\alpha = 1/5$, $a = 10$, and in the absence of ageing. *Left*: absolute values of the current. *Right*: non-normalised difference, the drop at around 2×10^3 is due to numerical issues. The power law (40) is shown in *red*. Both panels demonstrate that in the long time limit the width of the initial distribution is irrelevant

Fig. 5 Initial plateau value of the time-of-flight current in Ref. Schubert et al. (2013). The *red points* represent the experimental data and the *full line* is the best power law fit to Eq. (47), from which we find the scaling exponent $\alpha - 1 = -0.67$ is extracted, corresponding to $\alpha = 0.33$
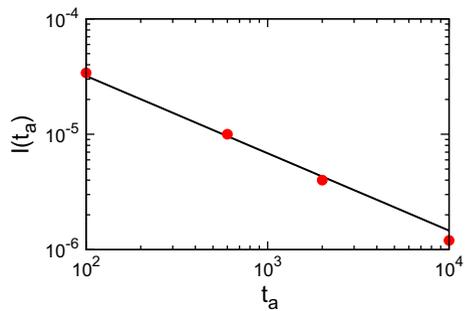
(Schubert et al. 2013). The charge carriers are created in a charge generation layer. The bias field is switched on only after an ageing period, and it is shown that the system can indeed be described by the CTRW statistics of the Scher–Montroll model. The experiment is repeated for different ageing times, and the measured curves are fitted to Monte Carlo simulations results based on the Scher–Montroll model. The fits to the simulations in Ref. Schubert et al. (2013) allow us to use their plateau values for comparison with Eq. (47). Figure 5 shows very good scaling of the experimental values, and from a least squares fit and comparison of the slope with Eq. (47) we obtain the anomalous diffusion exponent $\alpha = 0.33$. This also compares well with the value $\alpha = 0.38$ found in Ref. Schubert et al. (2013) from the slope of the current characteristic. Note that the crossover between the power laws and thus also the power law exponents of the current also change with the delay time, as predicted by our theory, as shown in Fig. 1. While the crossovers indeed occur at the value of the ageing time, the exponents cannot be read off from the data as the intervals between t_a and t_c are too short to see a reliable power law behaviour.

8 Discussion

We discussed the effect of ageing on the current characteristic of the classical Scher–Montroll transport. We showed that the ageing time represents a second relevant time scale in addition

to the characteristic crossover time of the non-aged Scher–Montroll transport. Depending on these time scales an additional intermediate time power law regime and an initial plateau behaviour of the Scher–Montroll current may emerge. Specifically, for short ageing times $t_a \ll t_c$ the current shows the regular Scher–Montroll regimes, following an initial constant regime for $t \ll t_a$ which is relevant only as long as the ageing time t_a is not too short. For long ageing times $t_a \gg t_a$ the three different regimes can be found, separated by the normal crossover time and the ageing time. If the ageing time is of order of the normal crossover time, the current crosses over directly to the last regime and the intermediate regime does not exist. In the long time limit $t \gg t_a$ all curves show the same power law behaviour. In particular, the plateau value connected to the constant velocity of the diffusing charge carriers in this initial regime has a power law dependence on the ageing time. We also demonstrated that there is no significant effect of a broad initial charge carrier distribution on the long time behaviour, as expected. We note that the power law regimes found for the first passage density previously (Krüsemann et al. 2014, 2015) are represented in the results derived here, as the first passage time contributes to the Scher–Montroll current through the time derivative of the survival probability, which enters the equations according to Eq. (23).

Our results may, in principle, be used in experiments to determine the age of an observed Scher–Montroll process from the crossover time and the different slopes. In a non-aged process the sum of the slopes is exactly -2 whereas in the aged case one finds different results, depending on the values of the crossover time t_c and the ageing time t_a. In turn, if the age is known the dependence of the initial plateau value of the Scher–Montroll current on the ageing time t_a can be used to determine the anomalous scaling exponent of the waiting time distribution as was shown here using experimental (Schubert et al. 2013). To clearly distinguish three different regimes in an experiment, the observation time should span about nine decades, as the crossovers are no sharp transitions. While this is likely not achievable in many experimental realisations, by sweeping the parameters it should be possible to explore different windows of the entire first passage distribution and thus observe all occurring power laws.

We stress again that while we discussed our results in the language of electrical charge carriers and currents, this model may equally be used for tracer dispersion in subsurface aquifers. Assume that a chemical tracer substance enters the aquifer and then diffuses in the porous environment. As long as there is no significant bias current in the soil, the free diffusion of the tracer corresponds to the ageing period discussed here. After some (ageing) time rainfall causes the build up of a hydraulic current and drives the tracer towards a catchment. The resulting current characteristic should display the same crossover behaviours as predicted here.

References

Akimoto, T., Barkai, E.: Aging generates regular motions in weakly chaotic systems. Phys. Rev. E **87**, 032915 (2013)

Allegrini, P., Bellazzini, J., Bramanti, G., Ignaccolo, M., Grigolini, P., Yang, J.: Scaling breakdown: a signature of aging. Phys. Rev. E. **66**, 015101 (2002)

Barkai, E.: Fractional Fokker–Planck equation, solution, and application. Phys. Rev. E **63**, 046118 (2001)

Barkai, E.: Aging in subdiffusion generated by a deterministic dynamical system. Phys. Rev. Lett. **90**, 104101 (2003)

Barkai, E., Cheng, Y.C.: Aging continuous time random walks. J. Chem. Phys. **118**, 6167 (2003)

Barkai, E., Garini, Y., Metzler, R.: Strange kinetics of single molecules in living cells. Phys. Today **65**, 29 (2012)

Bel, G., Barkai, E.: Weak ergodicity breaking in the continuous-time random walk. Phys. Rev. Lett. **94**, 240602 (2005)

Berkowitz, B., Scher, H.: Anomalous transport in random fracture networks. Phys. Rev. Lett. **79**, 4038 (1997)

Berkowitz, B., Scher, H., Silliman, S.E.: Anomalous transport in laboratory-scale, heterogeneous porous media. Water Resour. Res. **36**, 149 (2000)

Berkowitz, B., Klafter, J., Metzler, R., Scher, H.: Physical pictures of transport in heterogeneous media: advection dispersion, random walk, and fractional derivative formulations. Water Resour. Res. **38**, 1–9 (2002)

Berkowitz, B., Cortis, A., Dentz, M., Scher, H.: Modeling non-Fickian transport in geological formations as a continuous time random walk. Rev. Geophys. **44**, RG2003 (2006)

Bodrova, A., Chechkin, A.V., Cherstvy, A.G., Metzler, R.: Quantifying non-ergodic dynamics of force-free granular gases. Phys. Chem. Chem. Phys. **17**, 21791 (2015)

Bouchaud, J.P.: Weak ergodicity breaking and ageing in disordered systems. J. Phys. I (Paris) **2**, 1705 (1992)

Bouchaud, J.P., Georges, A.: Anomalous diffusion in disordered media: statistical mechanisms, models and physical applications. Phys. Rep. **195**, 12 (1990)

Brokmann, X., Hermier, J.P., Messin, G., Desbiolles, P., Bouchaud, J.P., Dahan, M.: Statistical aging and nonergodicity in the fluorescence of single nanocrystals. Phys. Rev. Lett. **90**, 120601 (2003)

Burov, S., Metzler, R., Barkai, E.: Aging and nonergodicity beyond the Khinchin theorem. Proc. Natl. Acad. Sci. USA **107**, 13228 (2010)

Caspi, A., Granek, R., Elbaum, M.: Enhanced diffusion in active intracellular transport. Phys. Rev. Lett. **85**, 5655 (2000)

Cherstvy, A.G., Metzler, R.: Population splitting, trapping, and non-ergodicity in heterogeneous diffusion processes. Phys. Chem. Chem. Phys. **15**, 20220 (2013)

Cherstvy, A.G., Metzler, R.: Ergodicity breaking and particle spreading in noisy heterogeneous diffusion processes. J. Chem. Phys. **14**, 144105 (2015)

Davies, B.: Integral Transforms and Their Applications, vol. 41. Springer Verlag New York Inc, New York (2002)

Di Rienzo, C., Piazza, V., Gratton, E., Beltram, F., Cardarelli, F.: Probing short-range protein Brownian motion in the cytoplasm of living cells. Nature Commun. **5**, 5891 (2014)

Donth, E.: The Glass Transition. Springer, Berlin (2001)

Edery, Y., Scher, H., Guadagnini, A., Berkowitz, B.: Origins of anomalous transport in heterogeneous media: structural and dynamic controls. Water Resour. Res. **50**, 1490 (2014)

Feller, W.: An Introduction to Probability Theory and its Applications, vol. 2. Wiley, New York (1971)

Freundlich, H., Krüger, D.: Anomalous diffusion in true solution. Trans. Faraday Soc. **31**, 906 (1935)

Godrèche, C., Luck, J.M.: Statistics of the occupation time of renewal processes. J. Stat. Phys. **104**, 489 (2001)

Golding, I., Cox, E.C.: Physical nature of bacterial cytoplasm. Phys. Rev. Lett. **96**, 098102 (2006)

Goychuk, I.: Viscoelastic subdiffusion: generalised Langevin equation approach. Adv. Chem. Phys. **150**, 187 (2012)

Habdas, P., Schaar, D., Levitt, A.C., Weeks, E.R.: Forced motion of a probe particle near the colloidal glass transition. EPL **67**, 477 (2004)

He, Y., Burov, S., Metzler, R., Barkai, E.: Random time-scale invariant diffusion and transport coefficients. Phys. Rev. Lett. **101**, 058101 (2008)

Henkel, M., Pleimling, M., Sanctuary, R. (eds.): Ageing and the Glass Transition. Springer, Berlin (2007)

Herzog, R.O., Polotzky, A.: Die Diffusion einiger Farbstoffe. Z. Physik. Chem. **87**, 449 (1914)

Honigmann, A., Müller, V., Hell, S.W., Eggeling, C.: STED microscopy detects and quantifies liquid phase separation in lipid membranes using a new far-red emitting fluorescent phosphoglycerolipid analogue. Faraday Disc. **161**, 77 (2013)

Jeon, J.H., Tejedor, V., Burov, S., Barkai, E., Selhuber-Unkel, C., Berg-Sørensen, K., Oddershede, L., Metzler, R.: In vivo anomalous diffusion and weak ergodicity breaking of lipid granules. Phys. Rev. Lett. **106**, 048103 (2011)

Jeon, J.H., Barkai, E., Metzler, R.: Noisy continuous time random walks. J. Chem. Phys. **139**, 121916 (2013)

Jeon, J.H., Leijnse, N., Oddershede, L., Metzler, R.: Anomalous diffusion and power-law relaxation of the time averaged mean square displacement in worm-like micellar solutions. New J. Phys. **15**, 045011 (2013)

Jeon, J.H., Chechkin, A.V., Metzler, R.: Scaled Brownian motion: a paradoxical process with a time dependent diffusivity for the description of anomalous diffusion. Phys. Chem. Chem. Phys. **16**, 15811 (2014)

Jung, Y.J., Barkai, E., Silbey, R.J.: Lineshape theory and photon counting statistics for blinking quantum dots: a Lévy walk process. Chem. Phys. **284**, 181 (2002)

Kepten, E., Bronshtein, I., Garini, Y.: Ergodicity convergence test suggests telomere motion obeys fractional dynamics. Phys. Rev. E **83**, 041919 (2011)

Kirchner, J.W., Feng, X., Neal, C.: Fractal stream chemistry and its implications for contaminant transport in catchments. Nature **403**, 524 (2000)

Krüsemann, H., Godec, A., Metzler, R.: First-passage statistics for aging diffusion in systems with annealed and quenched disorder. Phys. Rev. E **89**, 040101 (2014)

Krüsemann, H., Godec, A., Metzler, R.: Ageing first passage time density in continuous time random walks and quenched energy landscapes. J. Phys. A **48**, 285001 (2015)

Kursawe, J., Schulz, J.H.P., Metzler, R.: Transient aging in fractional Brownian and Langevin-equation motion. Phys. Rev. E **88**, 062124 (2013)

Lubelski, A., Sokolov, I.M., Klafter, J.: Nonergodicity mimics inhomogeneity in single particle tracking. Phys. Rev. Lett. **100**, 250602 (2008)

Magdziarz, M., Metzler, R., Szczotka, W., Zebrowski, P.: Correlated continuous-time random walks in external force fields. Phys. Rev. E **85**, 051103 (2012)

Mandelbrot, B.B., van Ness, J.W.: Fractional Brownian motions, fractional noises and applications. SIAM Rev. **10**, 422 (1968)

Manzo, C., van Zanten, T.S., Saha, S., Torreno-Pina, J.A., Mayor, S., Garcia-Parajo, M.F.: PSF decomposition of nanoscopy images via Bayesian analysis unravels distinct molecular organization of the cell membrane. Scientific Reports, vol. 4 (2014)

Metzler, R., Barkai, E., Klafter, J.: Anomalous diffusion and relaxation close to thermal equilibrium: a fractional Fokker–Planck equation approach. Phys. Rev. Lett. **82**, 3563–3567 (1999)

Metzler, R., Klafter, J.: The random walk's guide to anomalous diffusion: a fractional dynamics approach. Phys. Rep. **339**, 1 (2000)

Metzler, R., Klafter, J.: Boundary value problems for fractional diffusion equations. Phys. A **278**, 107 (2000)

Metzler, R., Jeon, J.H., Cherstvy, A.G., Barkai, E.: Anomalous diffusion models and their properties: non-stationarity, non-ergodicity, and ageing at the centenary of single particle tracking. Phys. Chem. Chem. Phys. **16**, 24128 (2014)

Monthus, C., Bouchaud, J.P.: Models of traps and glass phenomenology. J. Phys. A **29**, 3847 (1996)

Montroll, E.W., Weiss, G.H.: Random walks on lattices II. J. Math. Phys. **6**, 167 (1965)

Reverey, J.F., Jeon, J.H., Bao, H., Leippe, M., Metzler, R., Selhuber-Unkel, C.: Superdiffusion dominates intracellular particle motion in the supercrowded cytoplasm of pathogenic *Acanthamoeba castellanii*. Scientific Reports, vol. 5 (2015)

Richardson, L.F.: Atmospheric diffusion shown on a distance-neighbour graph. Proc. R. Soc. Lond. Ser. A **110**, 709–737 (1926)

Robert, R., Nguyen, T.H., Gallet, F., Wilhelm, C.: In vivo determination of fluctuating forces during endosome trafficking using a combination of active and passive microrheology. PLoS One **4**, e10046 (2010)

Scher, H., Montroll, E.: Anomalous transit-time dispersion in amorphous solids. Phys. Rev. B **15**, 2455 (1975)

Schubert, M., Preis, E., Blakesley, J.C., Pingel, P., Scherf, U., Neher, D.: Mobility relaxation and electron trapping in a donor/acceptor copolymer. Phys. Rev. B **87**, 024203 (2013)

Schulz, J.H.P., Barkai, E., Metzler, R.: Aging effects and population splitting in single-particle trajectory averages. Phys. Rev. Lett. **110**, 020602 (2013)

Schulz, J.H.P., Barkai, E., Metzler, R.: Aging renewal theory and application to random walks. Phys. Rev. X **4**, 011028 (2014)

Shlesinger, M.F.: Asymptotic solutions of continuous time random walks. J. Stat. Phys. **5**, 421 (1974)

Sibatov, R.T.: Statistical interpretation of transient current power-law decay in colloidal quantum dot arrays. Phys. Scr. **84**, 025701 (2011)

Sokolov, I.M., Klafter, J.: Field-induced dispersion in subdiffusion. Phys. Rev. Lett. **97**, 140602 (2006)

Szymanski, J., Weiss, M.: Elucidating the origin of anomalous diffusion in crowded fluids. Phys. Rev. Lett. **103**, 038102 (2009)

Tabei, S.M.A., Burov, S., Kim, H.J., Kuznetsov, A., Huynh, T., Jureller, J., Philipson, L.H., Dinner, A.R., Scherer, N.F.: Intracellular transport of insulin granules is a subordinated random walk. Proc. Natl. Acad. Sci. USA **110**, 4911 (2013)

Tejedor, V., Bénichou, O., Voituriez, R., Jungmann, R., Simmel, F., Selhuber-Unkel, C., Oddershede, L., Metzler, R.: Quantitative analysis of single particle trajectories: mean maximal excursion method. Biophys. J. **98**, 1364 (2010)

Weigel, A.V., Simon, B., Tamkun, M.M., Krapf, D.: Ergodic and nonergodic processes coexist in the plasma membrane as observed by single-molecule tracking. Proc. Natl. Acad. Sci. USA **108**, 6438 (2011)

Weiss, M., Elsner, M., Kartberg, F., Nilsson, T.: Anomalous subdiffusion is a measure for cytoplasmic crowding in living cells. Biophys. J. **87**, 3518 (2004)

Wolfram, S.: Mathematica: A System for Doing Mathematics by Computer. Addison Wesley Longman Publishing Co., Inc., Boston (1991)

Wong, I.Y., Gardel, M.L., Reichman, D.R., Weeks, E.R., Valentine, M.T., Bausch, A.R., Weitz, D.A.: Anomalous diffusion probes microstructure dynamics of entangled F-actin networks. Phys. Rev. Lett. **92**, 178101 (2004)

Xu, Q., Feng, L., Sha, R., Seemann, N.C., Chaikin, P.M.: Subdiffusion of a sticky particle on a surface. Phys. Rev. Lett. **106**, 228102 (2011)